Regenerative Therapy 11 (2019) 17–24

Contents lists available at ScienceDirect

Regenerative Therapy

journal homepage: http://www.elsevier.com/locate/reth

Original Article

Asperosaponin VI stimulates osteogenic differentiation of rat adipose-derived stem cells

Xingpo Ding [a], Wuyin Li [b], Dengshan Chen [a], Chuanwei Zhang [a], Lei Wang [a], Hong Zhang [c], Na Qin [c], Yongqiang Sun [b, *]

[a] Department of Pediatric Orthopaedics, Henan Luoyang Orthopedic Hospital (Henan Provincial Orthopedic Hospital), China
[b] Joint Department, Henan Luoyang Orthopedic Hospital (Henan Provincial Orthopedic Hospital), China
[c] Pharmacy Department, Henan Luoyang Orthopedic Hospital (Henan Provincial Orthopedic Hospital), China

ARTICLE INFO

Article history:
Received 11 November 2018
Received in revised form
14 February 2019
Accepted 20 March 2019

Keywords:
Asperosaponin VI
Adipose-derived stem cells
Osteogenic differentiation
Bone defects

ABSTRACT

In the aging population, the decrease on osteogenic differentiation resulted into a significant reduction in bone formation. Bone tissue engineering has been a successful technique for treatment of bone defects. It is reported that adipose-derived stem cells (ADSCs) have pluripotency to differentiate into adipocytes and osteoblasts. However little is revealed about the effect of the herbal medicine Asperosaponin VI (ASA VI) on ADSCs differentiation. In our study, we isolated and identified ADSCs from rats. We examined the effect of different concentrations of ASA VI in ADSCs on alkaline phosphatase (ALP) activity, calcium deposition, the expression of bone-related proteins and the release of inflammatory cytokines. Flow-cytometry assay showed ADSCs were highly expressed CD44 and CD105, but hardly expressed CD34 and CD45, suggesting ADSCs were successfully isolated for follow-up experiments. ALP activity examination and Alizarin red (AR) stain showed that ASA VI enhanced the ALP activity and promoted matrix mineralization in ADSCs. In addition, bone-related protein OCN and RUNX2, and Smad2/3 phosphorylation was upregulated after ASA VI treatment in ADSCs. ELISA results showed that ASA VI blocked the release of TNF-α, IL-6 and IL-1β in ADSCs. Considering this results, we concluded that ASA VI promotes osteogenic differentiation of ADSCs through inducing the expression of bone-related proteins. These findings enriched the function of ASA VI as a regenerative medicine and shed new light for the treatment of bone defects in clinical research.

1. Introduction

Bone is a specialized type of connective tissue composed of two different cells named as osteoblasts and osteoclasts [1]. Extensive bone defect results in delayed or impaired bone healing [2]. Some surgical procedures, including the Masquelet and Ilizarov technique, partly reconstruct some bone defects [3]. Bone remodeling is a dynamic metabolic process directed by the balance between bone-forming osteoblasts and bone-resorbing osteoclasts [4]. Bone constructs produced by tissue engineering technique has been introduced as a new strategy for treatment of bone defects [5]. Mesenchymal stem cells (MSCs) are multipotent cells with the potentials to differentiate into various tissues, such as osteoblasts and adipocytes [6], and are most frequently isolated from bone marrow and adipose tissues [7]. Adipose-derived stem cells (ADSCs) have been proposed as an ideal source for cell-based therapies to support bone regeneration due to due to its wide distribution through the body, easy access, less morbidity and a low risk of tumorigenesis [8].

Dipsaci Radix (Chinese named Xu Duan) is the dried root of a kind of perennial herb *Dipsacus asper Wall* growing in moist fields and mountain in China [9]. Previous studies showed that *Dipsaci Radix* contains triterpenoid saponins [10] and iridoid glucosides [11]. Asperosaponin VI (ASA VI, also named Akebia Saponin D) is a

Abbreviations: ASA VI, Asperosaponin VI; MSCs, mesenchymal stem cells; ADSCs, adipose-derived stem cells; RUNX2, runt-related transcription factor 2; OCN, osteocalcin; ALP, alkaline phosphatase; AR, alizarin red; PE, phycoerythrin.

* Corresponding author. Joint Department, Henan Luoyang Orthopedic Hospital (Henan Provincial Orthopedic Hospital), No. 100 yongping Road, zhengdong new district, zhengzhou, Henan, 471002, China.
E-mail address: sunyongqiangsyq@163.com (Y. Sun).

Peer review under responsibility of the Japanese Society for Regenerative Medicine.

https://doi.org/10.1016/j.reth.2019.03.007

typical bioactive triterpenoid saponin from *D. asper Wall* [12]. It is reported that ASA VI exerts apoptosis-inducing activity through the activation of apoptosis-related p53 and Bax expression [13]. Pharmacological study demonstrated that ASA VI promotes MC3T3-E1 and primary rat osteoblasts proliferation and enhanced the formation of bone nodules in osteoblast cells [14]. Some reports illustrated that stimulating factors are able to induce osteogenic differentiation of ADSCs [15]. However whether ASA VI could induce osteogenic differentiation of ADSCs remains elusive.

In our study, we isolated ADSCs from rat adipose tissues and performed surface antigen identification and differentiation potential analysis of ADSCs. We examined the application of ASA VI at different concentrations on ALP activity, calcium deposition, and the expression of bone-related proteins and the levels of inflammatory cytokines. Our results showed that ASA VI promotes bone-related gene expression to stimulate osteogenic differentiation of ADSCs, which provides a new strategy for the treatment of bone disorders. In addition, ASA VI increases the anti-inflammatory effect of ADSCs and is involved in calcification-inducing mechanism in ADSCs.

2. Materials and methods

2.1. Animal culture

A total of 20 SPF grade Sprague–Dawley (SD) rats, 4–6 months old, weighing 170–210 g were provided by Department of medicine, Nanchang University. Rats were kept at standard laboratory conditions at 18–25 °C with 12 h light: 12 h dark. Standard rodent feed and water were available ad libitum. All procedures were performed according to the Guide for the Humane Use and Care of Laboratory. This study was approved by the Animal Care Committee of Henan Luoyang Orthopedic Hospital (No. [2014] 036).

2.2. Isolation and culture of ADSCs

SD rats were anaesthetized with pentobarbital sodium (40 mg/kg). The fresh adipose tissues (about 1.5 mL) were isolated from SD rats in a sterile way, and minced into small pieces. After being digested with collagenase type I (1 g/L) at 37 °C for 75 min, the samples were filtered through 200 mesh filter net and centrifuged at 1200 rpm for 5 min. The supernatant was discarded and the resultant cell pellet was washed with sterile phosphate-buffered saline (PBS) to eliminate any contaminants. Cells were resuspended in Dulbecco's Modified Eagle Medium/Nutrient Mixture F-12 (DMEM/F12, 1:1, catalog: 1861453, GIBCO, USA) containing 10% fetal bovine serum (FBS, SKU: 04-007-1A, Biological Industries, Israel) and seeded into 25 cm^2 flask in an incubator at 37 °C with 5% CO_2. Fresh medium was added into cells twice a week. At the density of 80%–90%, ADSCs were digested with 0.25% trypsin for 3 min and passaged according to 1:2 ratios. ADSCs between passages III and V were used for the follow-up experiments.

2.3. Alizarin red (AR) stain analysis of ADSCs

ADSCs were seeded into a 6-well plate at the density of 3×10^4 cells/well in DMEM/F12 with 10% FBS for mineralization assay with AR Staining Kit (catalog: KGA363-1, KeyGEN BioTECH company, Nanjing, China). After 48 h, ADSCs were incubated with osteogenic induction medium (catalog: RASMD-90021, Cyagen biotechnology company, Suzhou, Jiangsu, China) containing 10 nM dexamethasone, 10 mM β-glycerophosphate, 50 μM ascorbate phosphate and 10% FBS. After 14 d, cells at the density of 90% were washed with PBS and fixed with 70% ethanol at room temperature for 1 h. After being washed with PBS, cells were incubated with 1% alizarin red solution at 37 °C for 1 h and captured. For the precipitation of alizarin red, these slides were incubated with 10% cetylpyridinium chloride for 30 min at room temperature. The calcium deposition was determined with a microplate spectrophotometer (SPECTRO star Nano, BMG Labtech, Germany) at the wavelength of 570 nm.

2.4. Oil red O staining

ADSCs were seeded into a 6-well plate at the density of 5×10^4 cells/well in DMEM/F12 with 10% FBS. After 48 h, cells were cultured with adipogenic induction medium containing 2% FBS, 1% antibiotic solution, 0.5 mM isobutyl-methylxanthine, 1 mM dexamethasone, 10 mM insulin and 200 mM indomethacin. After 14 d, cells were washed with PBS and fixed with 10% formalin for 5 min at room temperature. After washes, cells were incubated with Oil Red O staining solution (0.3%, Sigma, USA) for 15 min at room temperature. Images were observed with an inverted microscope Eclipse TS100 (Nikon, Tokyo, Japan).

2.5. Surface antigen identification of ADSCs

ADSCs were digested with 0.25% trypsin and suspended with PBS at the density of 2×10^6 cells/mL. A total of 50 μL cells were incubated for 20 min at 4 °C in the dark with 20 μL of the following antibodies: anti-CD105-phycoerythrin (PE; catalog: 550546), anti-CD44-PE (catalog: 561860), anti-CD34-PE (551387) and anti-CD45-phycoerythrin/CyChrome (PE/Cy5, catalog: 559135) (Becton, Dickinson and Company, USA). Then Cells were washed with flowcytometry buffer and analyzed with a Cyflow Space flowcytometer (Partec, Münster, Germany).

2.6. Detection of cell proliferation

The effect of ASA VI on the proliferation of ADSCs was evaluated using cell counting Kit-8 (CCK-8, Dojindo, Kyushu Island, Japan) according to the manufacture's protocol. ADSCs were seeded into 96-well plates at the density of 1×10^3 cells/well containing DMEM/F12 or asperosaponin VI (ASA VI, catalog: SA8570, Solarbio life sciences, Beijing, China) at various concentrations (10^{-7}, 10^{-6}, 10^{-5}, 10^{-4} or 0 M), with 6 replicate cells for each concentration. After 3, 7 or 14 d, each well was added 10 μL of CCK-8 solution and incubated in dark for 1 h at 37 °C. OD value was detected by a microplate reader (SPECTRO star Nano, BMG Labtech, Germany) at the wavelength of 450 nm.

2.7. Detection of alkaline phosphatase (ALP) activity

ADSCs were seeded into 96-well plates at the density of 1×10^4 cells/well and were randomly divided into six groups: Control, 0 M, 10^{-7} M, 10^{-6} M, 10^{-5} M and 10^{-4} M for ALP activity assay. Cells in Control group were incubated with DMEM/F12 containing 10% FBS for 3 d, 7 d, 14 d or 21 d, respectively. Cells in 0 M, 10^{-7} M, 10^{-6} M, 10^{-5} M or 10^{-4} M groups were cultured with osteogenic medium and 0 M, 10^{-7} M, 10^{-6} M, 10^{-5} M or 10^{-4} M ASA VI, respectively. At the density of 80%–90%, cells were lysed with 0.1% Triton X-100, and OD values were detected at the wavelength of 520 nm according to the manufacturer's protocol of ALP assay kit (catalog: A059-2, Nanjing Jiancheng Bioengineering Institute, Nanjing, China). ALP activity (U/gprot) = $(OD_{test}/OD_{standard})$ *$(\text{enzyme content})_{standard}/(\text{protein concentration})_{test}$.

2.8. Enzyme-linked immuno sorbent assay (ELISA)

The levels of OCN were determined by rat Osteocalcin/Bone gla protein ELISA assay kit (catalog: ml002883, mlbio elisakit producers, Shanghai, China) according to the manufacturer's protocol. Samples were diluted with phosphate buffered saline (PBS). The diluted sample was added into polystyrene plate at the density of 50 μL/well and incubated at 37 °C for 30 min. After being washed with wash buffer, the plate was incubated with fresh enzyme-labeled antibody for 1 h at 37 °C. After washes, the plate was incubated with chromogenic agents to develop color at 37 °C for 10 min in the dark. OD values were detected with a NanoDrop-2000 spectrophotometer at the wavelength of 450 nm with the blank control having an OD of zero.

2.9. Quantitative real-time polymerase chain reaction (qRT-PCR)

ADSCs were seeded into 6-well plate at the density of 1×10^5 cells/well. Cells in Control group were incubated with DMEM/F12 containing 10% FBS. Cells in 0 M, 10^{-7} M, 10^{-6} M, 10^{-5} M or 10^{-4} M groups were cultured with osteogenic medium with 0 M, 10^{-7} M, 10^{-6} M, 10^{-5} M or 10^{-4} M ASA VI, respectively. At the density of 80%–90%, total RNA was extracted from different groups using Trizol buffer (catalog: CW0580S, CWBIO, Beijing, China). The quality of RNA was determined by agarose electrophoresis, and the concentration was measured with a NanoDrop-2000 spectrophotometer at the absorbance of 260 nm and 280 nm. 0.5 μg RNA was reverse transcribed into cDNA with HiFiScript cDNA Synthesis Kit (catalog: CW2569M, CWBIO, Beijing, China) according to the instruction. The relative expression of target genes was detected in the Step-One real-time PCR system (Invitrogen, USA) using UltraSYBR Mixture (catalog: CW0957M, CWBIO, Beijing, China). The parameters for PCR were as follows: 95 °C for 5 min, followed by 40 cycles at 95 °C for 20 s and then at 60 °C for 20 s. The relative expression of RUNX2 and OCN was normalized to the internal control glyceraldehyde-phosphate dehydrogenase (GAPDH) using the $2^{-\Delta\Delta CT}$ method [16]. The primers for PCR were as follows: RUNX2 forward primer: 5′-caacttcctgtgctccgtg-3′, reverse primer: 5′-aagtgaaactcttgcctcgtc-3’; OCN forward primer: 5′-ggtgcagacctagcagacacca-3′, reverse primer: 5′-aggtagcgccggagtctattca-3’; GAPDH forward primer: 5′-caatgacccccttcattgacc-3′, reverse primer: 5′-gagaagcttcccgttctcag-3’.

2.10. Western blot

ADSCs were seeded into a 6-well plate at the density of 1×10^5 cells/well. Cells in Control group were incubated with DMEM/F12 containing 10% FBS. Cells in 0 M, 10^{-7} M, 10^{-6} M, 10^{-5} M or 10^{-4} M groups were cultured with osteogenic medium with 0 M, 10^{-7} M, 10^{-6} M, 10^{-5} M or 10^{-4} M ASA VI, respectively. After 14 d, proteins were extracted from different groups using RIPA buffer. The concentration was calculated with a bicinchoninic acid kit (Pierce, Germany) according to the manufacturer's protocol. An equal amount of protein was subjected onto SDS-PAGE and transferred to a polyvinylidene fluoride membrane (Millipore, Boston, MA, USA). After being blocked with 5% non-fat milk in Tris-buffered saline with 0.05% Tween 20 (TBST) for 1 h at room temperature, the membrane was incubated with rabbit polyclonal antibodies against OCN (1:800, catalog: A6205), RUNX2 (1:1,000, catalog: A6214) (Abclonal technology, USA), Smad2/3 (1:500, catalog: ab63672) and Smad2/3 (phospho T8) (1:1,000, catalog: ab63399) (Abcam, USA) at 4 °C overnight. The next morning, the membranes were washed with TBST and probed with the corresponding horseradish peroxidase-conjugated secondary antibody (1:10,000) for 1 h at room temperature. The signals were developed with an electrochemiluminescence solution (Pierce, Germany). The relative expression of RUNX2 and OCN were calculated by the normalization to GAPDH using Quantity One software v4.2 (Bio-Rad, USA).

2.11. Statistical analysis

All data were expressed as means ± standard deviation of three independent experiments. Statistical analysis was performed with SPSS software v17.0 (Chicago, IL, USA). Statistical correlation between two groups was performed using student *t*-test. The data were considered statistically significant when $P < 0.05$.

3. Results

3.1. ADSCs were successfully isolated from adipose tissues

As shown in Fig. 1A, ADSCs in primary culture displayed long spindle or fibroblast-like morphology. AR and oil O red staining showed that ADSC has pluripotency of osteogenic differentiation and adipose differentiation (Fig. 1B and C). Flow cytometry analysis of ADSCs showed that ADSCs positively expressed stem cell-associated markers CD44 (95.67%) and CD105 (96.88%), but weakly expressed hematopoietic cell marker CD34 and leukocyte marker CD45 (Fig. 1D–G). These data indicated that ADSCs were successfully isolated from adipose tissues and were capable of multi-lineage differentiation.

3.2. ASA VI did not affect ADSCs proliferation

In order to explore the effect of ASA VI on the proliferation of ADSCs, we incubated ADSCs at various concentration of ASA VI and performed CCK-8 assay. In Fig. 2, after 3 d incubation of ASA VI, there was no significant difference on OD value among Control, 0 M, 10^{-7} M, 10^{-6} M, 10^{-5} M and 10^{-4} M groups ($P > 0.05$). The similar results were observed after 7 and 14 d induction of ASA VI. There data showed that ASA VI at these concentrations had no effect on ADSCs proliferation.

3.3. ASA VI enhanced the ALP activity and calcium deposition

In order to explore the function of ASA VI on the osteogenic differentiation of ADSCs, we performed ALP activity assay and AR staining. In Fig. 3A, there was no significant difference among Control, 0 M, 10^{-7} M and 10^{-6} M groups after 3 d of ASA VI induction ($P > 0.05$); Compared with 0 M, ASA VI at the concentration of 10^{-5} M and 10^{-4} M of ASA VI significantly promoted the ALP activity ($P < 0.05$). At 7 d, 14 d and 21 d of induction, compared with Control group, ALP activity in 0 M group was significantly improved ($P < 0.05$). And the ALP activity at 10^{-7} M, 10^{-6} M, 10^{-5} M and 10^{-4} M groups was higher than that in 0 M group ($P < 0.05$) with the trend of 10^{-7} M < 10^{-6} M < 10^{-5} M < 10^{-4} M.

We employed AR stain to detect the effect of ASA VI on calcium deposition after 14 induction in Fig. 3B and C. Compared with Control group, the number of mineralized nodules marked in red in 0 M group was significantly increased in Fig. 3A ($P < 0.05$). The continuous treatment of ASA VI at 10^{-7} M, 10^{-6} M, 10^{-5} M and 10^{-4} M obviously increased the number of mineralized nodules, with the trend: 10^{-4} M > 10^{-5} M > 10^{-6} M > 10^{-7} M ($P < 0.05$). The similar results were observed in the content of calcium deposition in Fig. 3C. These data showed that ASA VI enhanced ALP activity and calcium deposition in ADSCs.

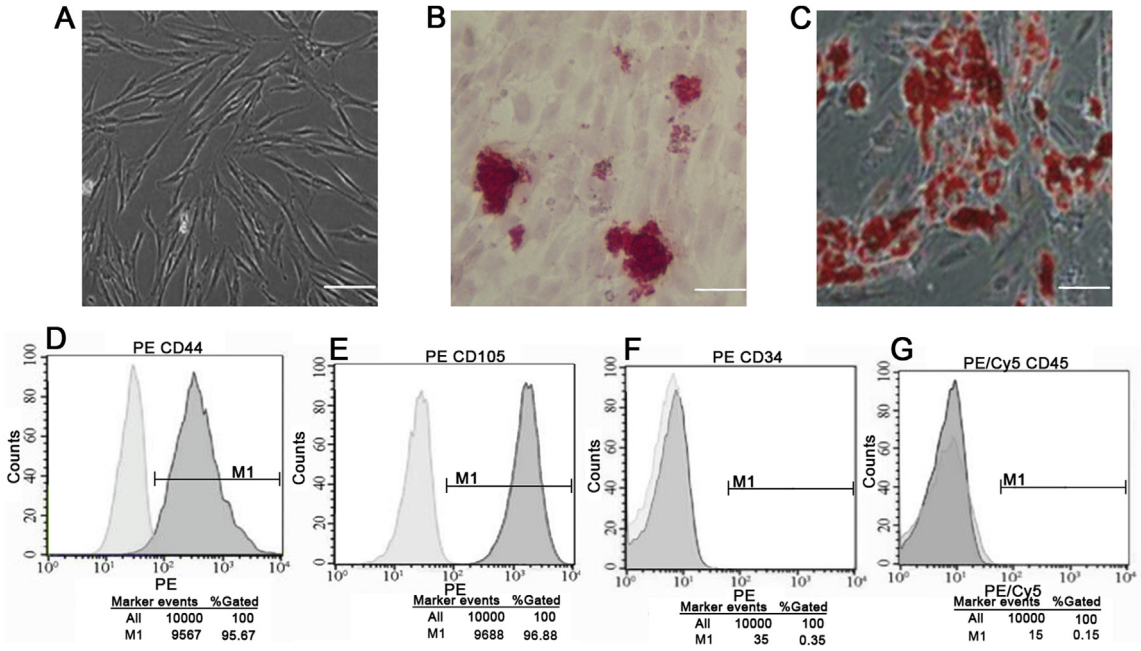

Fig. 1. ADSCs were successfully isolated from rat adipose tissues. A. ADSCs displayed fibroblast-like spindle shape. B. ADSCs were stained with AR. C. ADSCs were stained with Oil O red. Scale bar = 100 μm. B. ADSCs were highly expressed CD44 and CD105, but hardly expressed CD34 and CD45 detected by flowcytometry.

3.4. ASA VI promoted the expression of RUNX2 and OCN

We examined the level of OCN in ASA VI-induced ADSCs in Fig. 4A. No significant difference was observed among Control, 0 M, 10^{-7} M and 10^{-6} M groups at 3 d ($P > 0.05$). Compared with 0 M, the incubation of ASA VI at 10^{-5} M and 10^{-4} M enhanced the levels of OCN ($P < 0.05$). However, at 7 d, 14 d, and 21 d, the levels of OCN in 0 M were significantly higher than those in Control group ($P < 0.05$). And the addition of ASA VI at 10^{-7} M, 10^{-6} M, 10^{-5} M and 10^{-4} M obviously increased the levels of OCN. These data showed that ASA VI incubation promoted the expression of OCN.

We further investigated the mRNA and protein levels of RUNX2 and OCN after ASA VI induction. In Fig. 4B, the mRNA expression of OCN and RUNX2 in 0 M group was significantly higher than those in Control group ($P < 0.05$). And the addition of ASA VI at 10^{-7} M, 10^{-6} M, 10^{-5} M and 10^{-4} M improved the mRNA levels of OCN and RUNX2 ($P < 0.05$). The similar trends on the protein levels of OCN and RUNX2 were detected in Fig. 4C and D. These results showed that ASA VI enhanced the expression of OCN and RUNX2 in ADSCs.

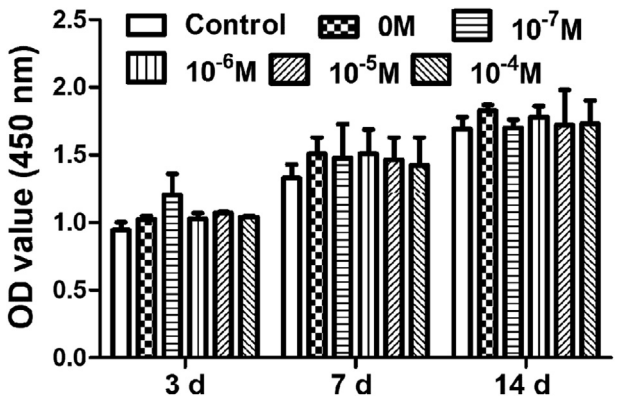

Fig. 2. ASA VI did not affect the proliferation of ADSCs. ADSCs were randomly divided into six groups: Control, 0 M, 10^{-7} M, 10^{-6} M, 10^{-5} M and 10^{-4} M. Cells in Control group was incubated with DMEM/F12 containing 10% FBS or different concentrations of ASA VI (0 M, 10^{-7} M, 10^{-6} M, 10^{-5} M or 10^{-4} M). OD value at the wavelength of 450 nm was detected with CCK-8 kit after 3, 7 or 14 d induction.

3.5. ASA VI blocked the release of pro-inflammatory cytokines in ADSCs

We examined the levels of TNF-α, IL-6 and IL-1β after the induction of ASA VI in ADSCs. In Fig. 5A–C, compared with 0 M group, the addition of ASA VI significantly blocked the levels of TNF-α, IL-6 and IL-1β ($P < 0.05$), suggesting that ASA VI exerted the anti-inflammatory effect in ADSCs. To explore the calcification-inducing mechanism of ASA VI in ADSCs, we examined the effect of ASA VI on Smad2/3 phosphorylation. In Fig. 5D, no significant difference was observed between Control and 0 M groups ($P > 0.05$). However, compared with 0 M group, the application of ASA VI significantly increased Smad2/3 phosphorylation, suggesting that ASA VI promotes Smad2/3 phosphorylation in ADSCs.

4. Discussion

In the aging population, osteogenic differentiation of MSCs decreases, leading to a significant reduction in bone formation [17]. In addition, alterations in bone mass and quality caused by osteoporosis and obesity are major health problems worldwide [18]. Bone tissue engineering has developed a new strategy for treatment of bone disorders [3].

Bone remodeling is a result of the balanced bone formation by osteoblasts and bone resorption by osteoclasts [19]. MSCs have the potentials to differentiate into chondrocytes, adipocyte and osteoblasts and are introduced as a suitable candidate for bone regenerative techniques [20]. ADSCs can be induced to differentiate into mesenchymal lineages, such as adipocytes, osteoblasts and chondrocytes [21]. Previous study revealed that extremely low frequency pulsed electromagnetic fields improves osteogenic differentiation of human ADSCs [3,22,23], indicating the potential of ADSCs differentiation into

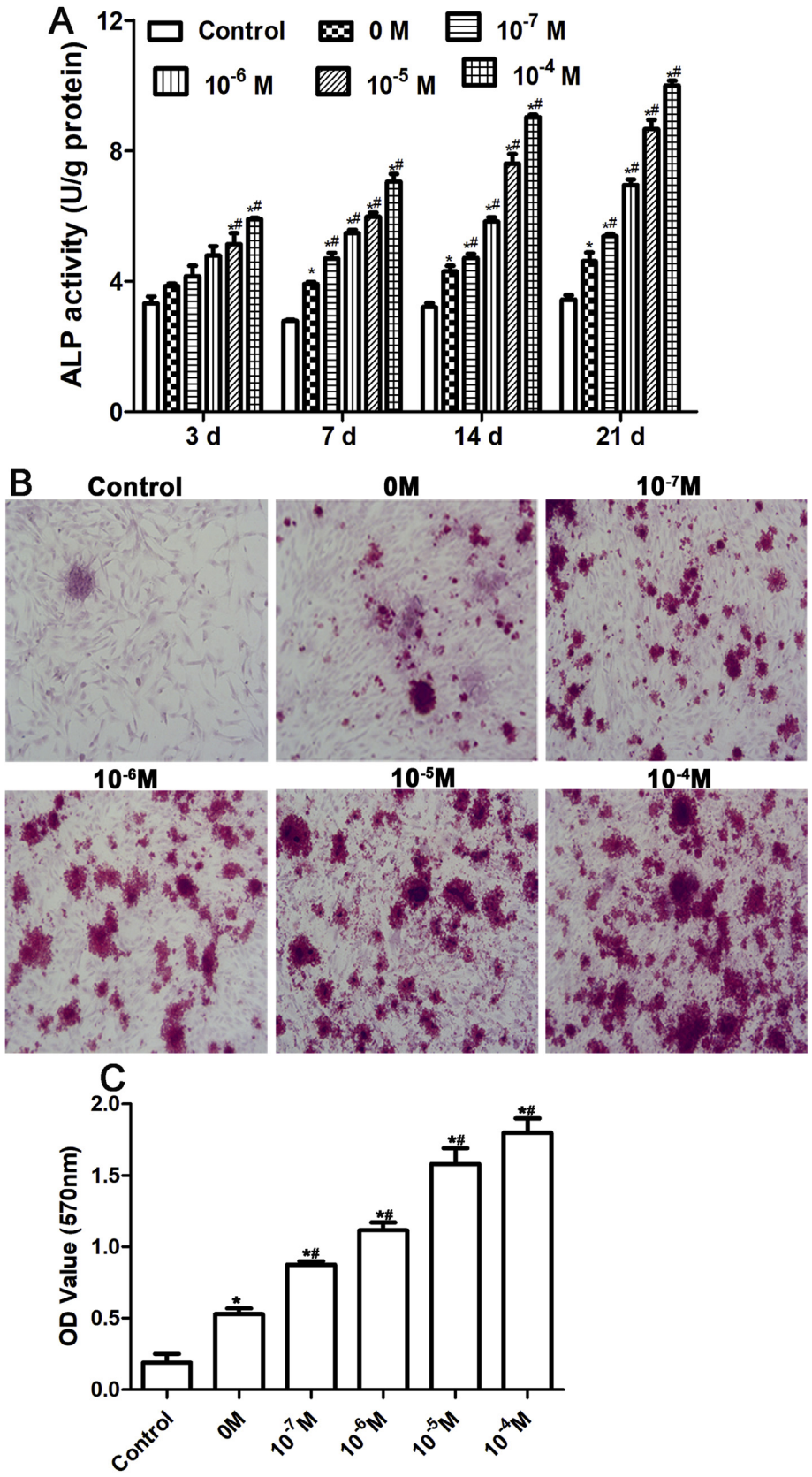

Fig. 3. ASA VI enhanced ALP activity and calcium deposition in ADSCs. ADSCs were randomly divided into six groups: Control, 0 M, 10^{-7} M, 10^{-6} M, 10^{-5} M and 10^{-4} M. Cells in Control group was incubated with DMEM/F12 containing 10% FBS. Cells in 0 M, 10^{-7} M, 10^{-6} M, 10^{-5} M or 10^{-4} M were cultured with osteogenic medium containing ASA VI at the concentration of 0 M, 10^{-7} M, 10^{-6} M, 10^{-5} M or 10^{-4} M, respectively. **A. ALP activity was detected determined at the wavelength of 520 nm.** ALP activity (U/gprot) = $(OD_{test}/OD_{standard})^*(\text{enzyme content})_{standard}/(\text{protein concentration})_{test}$. **B. ADSCs were stained with AR. C. Calcium deposition was determined at the wavelength of 570 nm**$^*P < 0.05$, compared with Control group; $^{\#}P < 0.05$, compared with 0 M group.

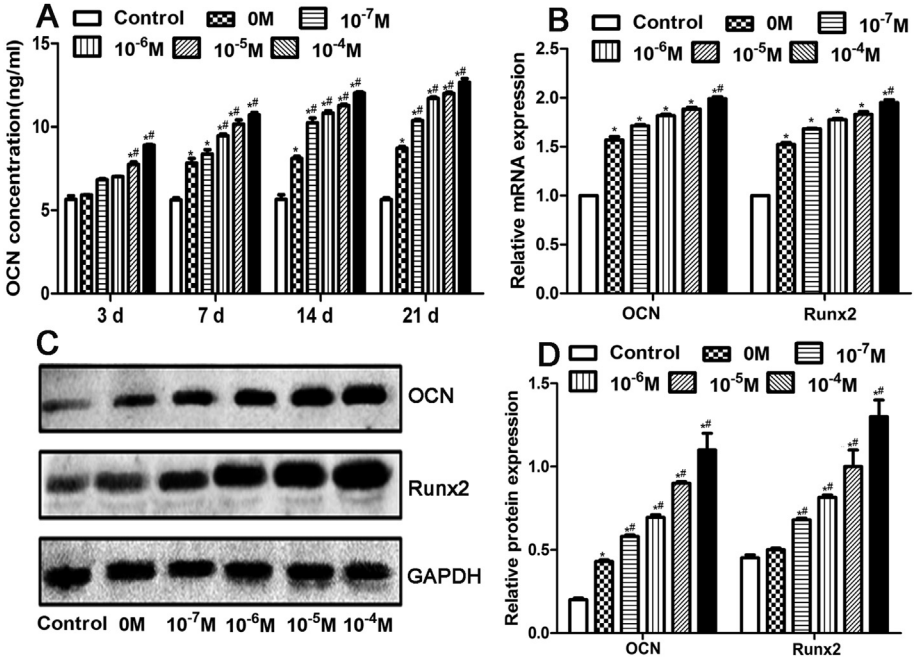

Fig. 4. ASA VI promoted the expression of OCN and RUNX2. ADSCs were divided into 6 groups. Cells in Control group were incubated with DMEM/F12 containing 10% FBS. Cells in 0 M, 10^{-7} M, 10^{-6} M, 10^{-5} M or 10^{-4} M groups were cultured with osteogenic medium with 0 M, 10^{-7} M, 10^{-6} M, 10^{-5} M or 10^{-4} M ASA VI, respectively. **A. ASA VI increased the levels of OCN detected by ELISA.** After 3 d, 7 d, 14 d or 21 d induction, medium was collected for ELISA. **B. ASA VI enhanced the mRNA levels of OCN and RUNX2 examined by qRT-PCR.** After 14 d, total RNA was extracted for qRT-PCR. The relative mRNA expression of OCN and RUNX2 was normalized to GAPDH with the method of $2^{-\Delta\Delta CT}$. **C and D, ASA VI upregulated the protein levels of OCN and RUNX2 determined by western blot.** After 14 d, protein was isolated for western blot. GAPDH was employed as the internal control. *P < 0.05, compared with Control group; #P < 0.05, compared with 0 M group.

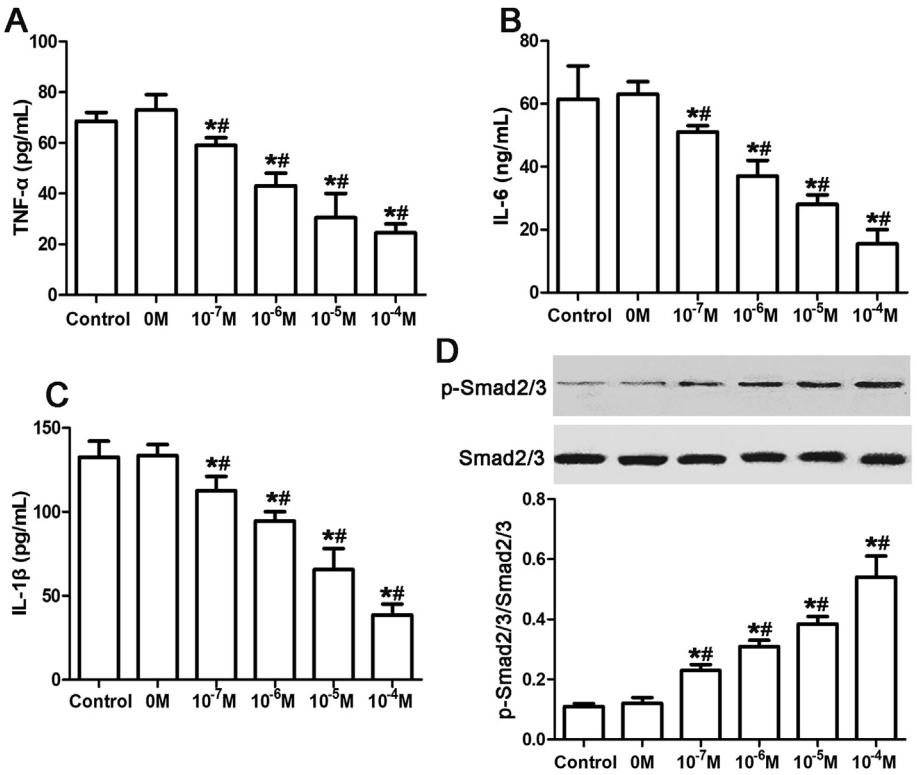

Fig. 5. ASA VI affected the release of inflammatory cytokines and smad2/3 phosphorylation. ADSCs were divided into 6 groups. Cells in Control group were incubated with DMEM/F12 containing 10% FBS. Cells in 0 M, 10^{-7} M, 10^{-6} M, 10^{-5} M or 10^{-4} M groups were cultured with osteogenic medium with 0 M, 10^{-7} M, 10^{-6} M, 10^{-5} M or 10^{-4} M ASA VI, respectively. After 14 d, the levels of TNF-α (A), IL-6 (B) and IL-1β (C) were detected with ELISA. D. Smad2/3 phosphorylation was blocked after ASA VI induction in ADSCs. After 14 d, proteins were collected for western blot. *P < 0.05, compared with Control group; #P < 0.05, compared with 0 M group.

osteoblasts. ADSCs have attracted much interest in the field of tissue engineering because of their easy access, less discomfort and great number of stem cells [24]. In our study, we found calcium deposition and lipid droplets via AR analysis and oil red O stain in Fig. 1B and C, which indicated the capacity of ADSCs to differentiate to osteoblast and adipocyte lineages. CD44 and CD105 displayed positive and CD34 and CD45 displayed negative in Fig. 1D–G. Thus, ADSCs displayed fibroblast-like morphology but have the capacity of differentiation, which provided a good model for our research.

Specific transcription factors such as RUNX2 is involved in the regulation of osteogenic differentiation, and controls the expression of bone extracellular matrix proteins by binding to various bone-specific targets such as ALP and OCN [29,30]. OCN acts as the most abundant glycoprotein in bone extracellular matrix via binding to calcium ions and regulates the mineralization of bone matrix [31]. ALP activity is a phenotypic marker for the early and mature osteoblasts [25]. The formation of mineralized nodules is one of the markers of osteoblastic maturation [26]. ASA VI is the main pharmacologically active constituent derived from Dipsacus asper Wall [12], which has long been used as a tonic and anti-inflammatory agent in traditional Chinese medicine for the therapy of bone fractures [27,28]. In our study, we found that different concentrations of ASA VI incubation in ADSCs significantly enhanced the ALP activity and the content of calcium deposition. In addition, ASA VI upregulated the mRNA and protein levels of OCN and RUNX2 in ADSCs. Considering these data, we concluded that ASA VI promotes the osteogenic differentiation of ADSCs via inducing the expression of bone-related proteins such as RUNX2 and OCN. In addition, we found that the application of ASA VI significantly blocked the release of pro-inflammatory cytokines such as IL-6 and IL-1β, indicating that ASA VI exerted anti-inflammatory effect in ADSCs. These data provided new evidence about ASA VI used as anti-inflammatory agent [27,28]. Previous study showed that ADSCs exerts regenerative effect by anti-inflammatory effect [29]. That's to say, the application of ASA VI in ADSCs increases the anti-inflammatory effect of ADSCs and promotes the regenerative effect.

ASA VI has been developed as a new drug to treat osteoporosis and granted a Chinese patent by Zhejiang Dier Pharmaceutical Co. Ltd [30]. It is reported that Dipsacus asper Wall induced osteoblastic differentiation through a bone morphogenic protein-2/mitogen-activated protein kinase/SMAD/1/5/8-dependent runt-related transcription factor 2 signaling pathway [31]. It is also indicated that ASA VI promotes MC3T3-E1 and primary rat osteoblasts proliferation and enhanced the formation of bone nodules in osteoblast cells [14]. Smad2/3 is the major component of transforming growth factor-β (TGF-β) and is closely associates with the regulation of bone formation [32]. In our study, we found that the addition of ASA VI increased the Smad2/3 phosphorylation, which is in agreement with the previous study. These data showed that ASA VI might promote osteogenic differentiation of ADSCs via TGF-β/smad pathway. However, more experiments need to be performed to explore the exact mechanism.

Although the potential of ADSCs and the function of ASA VI on osteoblasts were reported separately, little was referred to the effect of ASA VI on ADSCs differentiation. In our study, we combined ASA VI and ADSCs and found that the addition of ASA VI significantly promoted the osteogenic differentiation of ADSCs. Based on the attractive characteristics of ADSCs for clinical application and the widespread of ASA VI, our findings provided a new insight for bone modeling with higher efficacy, less side effects and lower costs.

5. Conclusion

In our study, we found that ASA VI had no effect on cell proliferation, enhanced the ALP activity and calcium deposition, upregulated the levels of RUNX2 and OCN, blocked the release of TNF-α, IL-6 and IL-1β, but promoted the phosphorylation of Smad2/3 in ADSCs. These data showed that ASA VI stimulated osteogenic differentiation of ADSCs through inducing the expression of RUNX2 and OCN. These findings enriched the function of ASA VI and provided a new insight for bone modeling with higher efficacy, less side effects and lower costs. We also found that ASA VI affected the expression of inflammatory cytokines and the phosphorylation of Smad2/3 in ADSCs, however, more extensive investigations need to be carried out to explore the underlying mechanisms of ASA VI promoting ADSCs osteogenic differentiation.

Fund

This study was supported by Special subject of Chinese medicine research in Henan in 2014 (No. 2014ZY02039).

Conflicts of interest

All authors declare no conflict of interest.

Appendix A. Supplementary data

Supplementary data to this article can be found online at https://doi.org/10.1016/j.reth.2019.03.007.

References

[1] Zhang JF, Li G, Chan CY, Meng CL, Lin MC, Chen YC, et al. Flavonoids of Herba Epimedii regulate osteogenesis of human mesenchymal stem cells through BMP and Wnt/beta-catenin signaling pathway. Mol Cell Endocrinol 2010;314:70–4.
[2] Smith JO, Aarvold A, Tayton ER, Dunlop DG, Oreffo RO. Skeletal tissue regeneration: current approaches, challenges, and novel reconstructive strategies for an aging population. Tissue Eng B Rev 2011;17:307–20.
[3] Ehnert S, van Griensven M, Unger M, Scheffler H, Falldorf K, Fentz AK, et al. Co-culture with human osteoblasts and exposure to extremely low frequency pulsed electromagnetic fields improve osteogenic differentiation of human adipose-derived mesenchymal stem cells. Int J Mol Sci 2018;19.
[4] Choi YH, Han Y, Jin SW, Lee GH, Kim GS, Lee DY, et al. Pseudoshikonin I enhances osteoblast differentiation by stimulating Runx2 and Osterix. J Cell Biochem 2018;119:748–57.
[5] Dawson JI, Kanczler J, Tare R, Kassem M, Oreffo RO. Concise review: bridging the gap: bone regeneration using skeletal stem cell-based strategies - where are we now? Stem Cell 2014;32:35–44.
[6] Dominici M, Le Blanc K, Mueller I, Slaper-Cortenbach I, Marini F, Krause D, et al. Minimal criteria for defining multipotent mesenchymal stromal cells. The International Society for Cellular Therapy position statement. Cytotherapy 2006;8:315–7.
[7] Granero-Molto F, Weis JA, Longobardi L, Spagnoli A. Role of mesenchymal stem cells in regenerative medicine: application to bone and cartilage repair. Expert Opin Biol Ther 2008;8:255–68.
[8] Wei X, Yang X, Han ZP, Qu FF, Shao L, Shi YF. Mesenchymal stem cells: a new trend for cell therapy. Acta Pharmacol Sin 2013;34:747–54.
[9] Tian XY, Wang YH, Liu HY, Yu SS, Fang WS. On the chemical constituents of Dipsacus asper. Chem Pharm Bull (Tokyo) 2007;55:1677–81.
[10] Jung KY, Do JC, Son KH. Triterpene glycosides from the roots of Dipsacus asper. J Nat Prod 1993;56:1912–6.
[11] Tomita H, Mouri Y. An iridoid glucoside from dipsacus asperoides. Phytochemistry 1996;42:239–40.
[12] Wu Y, Ji D, Liu Y, Zhang C, Yang Z. Industrial-scale preparation of akebia saponin D by a two-step macroporous resin column separation. Molecules 2012;17:7798–809.
[13] Jeong SI, Zhou B, Bae JB, Kim NS, Kim SG, Kwon J, et al. Apoptosis-inducing effect of akebia saponin D from the roots of Dipsacus asper Wall in U937 cells. Arch Pharm Res 2008;31:1399–404.

[14] Suh H, Song D, Huh S, Son K, Kim Y. Antinociceptive mechanisms of dipsacus saponin C administered intrathecally in mice. J Ethnopharmacol 2000;71:211–8.
[15] Guerado E, Caso E. Challenges of bone tissue engineering in orthopaedic patients. World J Orthoped 2017;8:87–98.
[16] Schmittgen TD, Livak KJ. Analyzing real-time PCR data by the comparative C(T) method. Nat Protoc 2008;3:1101–8.
[17] Chen XD, Shi S, Xu T, Robey PG, Young MF. Age-related osteoporosis in biglycan-deficient mice is related to defects in bone marrow stromal cells. J Bone Miner Res 2002;17:331–40.
[18] Picke AK, Campbell GM, Schmidt FN, Busse B, Rauner M, Simon JC, et al. Thy-1 deficiency augments bone loss in obesity by affecting bone formation and resorption. Front Cell Dev Biol 2018;6:127.
[19] Crockett JC, Rogers MJ, Coxon FP, Hocking LJ, Helfrich MH. Bone remodelling at a glance. J Cell Sci 2011;124:991–8.
[20] Rada T, Reis RL, Gomes ME. Adipose tissue-derived stem cells and their application in bone and cartilage tissue engineering. Tissue Eng B Rev 2009;15:113–25.
[21] Carbone A, Valente M, Annacontini L, Castellani S, Di Gioia S, Parisi D, et al. Adipose-derived mesenchymal stromal (stem) cells differentiate to osteoblast and chondroblast lineages upon incubation with conditioned media from dental pulp stem cell-derived osteoblasts and auricle cartilage chondrocytes. J Biol Regul Homeost Agents 2016;30:111–22.
[22] Yin Y, Chen P, Yu Q, Peng Y, Zhu Z, Tian J. The effects of a pulsed electromagnetic field on the proliferation and osteogenic differentiation of human adipose-derived stem cells. Med Sci Mon Int Med J Exp Clin Res 2018;24:3274–82.
[23] Orbay H, Busse B, Leach JK, Sahar DE. The effects of adipose-derived stem cells differentiated into endothelial cells and osteoblasts on healing of critical size calvarial defects. J Craniofac Surg 2017;28:1874–9.
[24] Kasir R, Vernekar VN, Laurencin CT. Regenerative engineering of cartilage using adipose-derived stem cells. Regen Eng Transl Med 2015;1:42–9.
[25] Li K, Xiu C, Zhou Q, Ni L, Du J, Gong T, et al. A dual role of cholesterol in osteogenic differentiation of bone marrow stromal cells. J Cell Physiol 2019;234:2058–66.
[26] Jiang M, Wang T, Yan X, Liu Z, Yan Y, Yang K, et al. A novel rhein derivative modulates bone formation and resorption and ameliorates oestrogen-dependent bone loss. J Bone Miner Res 2019;34:361–74.
[27] Peng LH, Ko CH, Siu SW, Koon CM, Yue GL, Cheng WH, et al. In vitro & in vivo assessment of a herbal formula used topically for bone fracture treatment. J Ethnopharmacol 2010;131:282–9.
[28] Niu Y, Li Y, Huang H, Kong X, Zhang R, Liu L, et al. Asperosaponin VI, a saponin component from Dipsacus asper wall, induces osteoblast differentiation through bone morphogenetic protein-2/p38 and extracellular signal-regulated kinase 1/2 pathway. Phytother Res 2011;25:1700–6.
[29] Kotani T, Masutani R, Suzuka T, Oda K, Makino S, Ii M. Anti-inflammatory and anti-fibrotic effects of intravenous adipose-derived stem cell transplantation in a mouse model of bleomycin-induced interstitial pneumonia. Sci Rep 2017;7:14608.
[30] Li K, Ding L, Yang ZL, Liu EH, Qi LW, Li P, et al. Determination of asperosaponin VI in rat plasma by HPLC-ESI-MS and its application to preliminary pharmacokinetic studies. Biomed Chromatogr 2010;24:550–5.
[31] Niu YB, Kong XH, Li YH, Fan L, Pan YL, Li CR, et al. Radix Dipsaci total saponins stimulate MC3T3-E1 cell differentiation via the bone morphogenetic protein-2/MAPK/Smad-dependent Runx2 pathway. Mol Med Rep 2015;11:4468–72.
[32] Heo SY, Ko SC, Nam SY, Oh J, Kim YM, Kim JI, et al. Fish bone peptide promotes osteogenic differentiation of MC3T3-E1 pre-osteoblasts through upregulation of MAPKs and Smad pathways activated BMP-2 receptor. Cell Biochem Funct 2018;36:137–46.